Acta Crystallographica Section F
Structural Biology and Crystallization Communications
ISSN 1744-3091

A preliminary X-ray study of human nucleoside diphosphate kinase A under oxidative conditions

Mi-Sun Kim, Jihye Jeong, Kong-Joo Lee and Dong Hae Shin*

College of Pharmacy, Division of Life and Pharmaceutical Sciences, Ewha Womans University, Seoul 120-750, Republic of Korea

Correspondence e-mail: dhshin55@ewha.ac.kr

Received 29 May 2010
Accepted 7 September 2010

Nucleoside diphosphate kinase (NDPK) catalyzes transfer of the γ-phosphoryl group from a nucleoside triphosphate (NTP) to a nucleoside diphosphate. The high-energy phosphate for this reaction is usually supplied by ATP. NDPK plays a primary role not only in maintaining cellular pools of all NTPs but also in the regulation of important cellular processes. NDPK-A (or Nm23-H1), one of eight human NDPKs, acts as a metastasis suppressor for some tumour types. A recent study showed that homohexameric human NDPK-A is regulated in response to oxidative stress. The activity of NDPK-A is reduced, with a concomitant increase in the population of dimeric NDPK-A, under oxidative conditions. In this study, human NDPK-A has been crystallized under oxidative conditions and X-ray data have been collected to 2.80 Å resolution using synchrotron radiation. The crystal belonged to the primitive cubic space group $P2_13$, with unit-cell parameters $a = b = c = 106.8$ Å. There is one NDPK-A dimer in the asymmetric unit. The preliminary electron-density map shows a large conformational change of the C-terminal domain of NDPK-A induced by a novel disulfide bond that is formed under oxidative conditions.

1. Introduction

Nucleoside diphosphate kinase (NDPK) is a multifunctional protein with a key enzymatic function, nucleotide transphosphorylation, which regulates the cellular pools of all nucleoside triphosphates (Rosengard *et al.*, 1989). NDPK is also known as Nm23 (nonmetastatic 23 protein) owing to its metastasis suppressor activity in some tumour types. Its enzymatic activity is also coupled to modulation of signal transduction by a diverse set of growth factors, such as transforming growth factor β1 (TGF-β1), nerve growth factor, platelet-derived growth factor and insulin-like growth factor 1 through unknown mechanisms (Otero, 2000). There are eight known NDPK genes in the human genome (Ishikawa *et al.*, 2003). A recent study of NDPK-A (or Nm23-H1), one of these gene products, showed that its biological function as a housekeeping enzyme and as a tumour metastasis suppressor is redox-regulated at Cys109 near the active site (Lee *et al.*, 2009). This cysteine residue is oxidized to various oxidation states, including disulfide cross-links, glutathionylation and sulfonic acid formation, in response to H_2O_2 treatment. Intermolecular Cys109–Cys109 disulfide bridges have also been detected using mass spectrometry (Song *et al.*, 2000). These modifications inhibited the NDPK enzymatic activity of Nm23-H1 as well as its metastatic suppressor activity. The disulfide cross-links of NDPK-A are substrates of the NADPH–TrxR1–thioredoxin shuttle system and enzymatic activity is recovered by the system.

The crystal structure of native human NDPK-A revealed a homohexameric structure stabilized by cross-interaction between the Kpn loop region and the neighbouring C-terminal domain (Min *et al.*, 2002). However, a large proportion of the native homohexameric form of NDPK-A with full NDPK activity disappears upon disulfide cross-linking, with a concomitant increase in the inactive dimeric form (Song *et al.*, 2000). Therefore, a tertiary conformational change

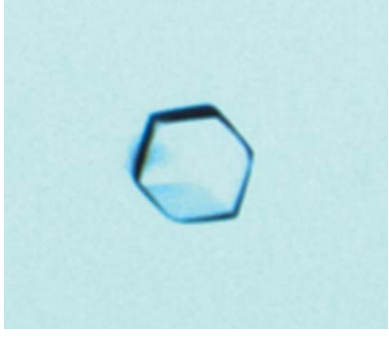

Table 1
Data-collection statistics.

Values in parentheses are for the highest resolution shell.

X-ray source	Pohang Light Source beamline 4A
X-ray wavelength (Å)	1.000
Temperature (K)	100
Space group	$P2_13$
Unit-cell parameters (Å)	$a = b = c = 106.8$
Volume fraction of solvent (%)	56.4
V_M (Å^3 Da^{-1})	2.82
Resolution range (Å)	50.0–2.80 (2.95–2.80)
Unique reflections	10205 (1457)
Multiplicity	15.3 (15.8)
R_{merge}† (%)	17.3 (57.7)
R_{meas}‡ (%)	17.9 (59.6)
Data completeness (%)	99.9 (100)
Average $I/\sigma(I)$	4.1 (1.3)

† $R_{merge} = \sum_{hkl}\sum_i |I_i(hkl) - \langle I(hkl)\rangle| / \sum_{hkl}\sum_i I_i(hkl)$. ‡ R_{meas} is the redundancy-independent R_{merge}.

of NDPK-A that influences its quaternary state under oxidative conditions seems to strongly regulate its enzymatic activity. However, the crystal structure of oxidized NDPK-A is not yet available. In order to elucidate the structural and functional relationship during the oxido-reduction cycle, we have initiated the determination of the three-dimensional structure of NDPK-A under oxidative conditions. Here, we report the crystallization and preliminary X-ray study of oxidized human NDPK-A.

2. Experimental methods

2.1. Crystallization

Human NDPK-A was cloned, overproduced and purified as described previously (Song *et al.*, 2000). The purified protein was concentrated to 10 mg ml^{-1} for crystallization. In cells, a 10 µ*M* H_2O_2 concentration is sufficient to induce oxidative stress (Stone & Yang, 2006). However, *in vitro*, a 5 m*M* H_2O_2 concentration was not sufficient to produce fully oxidized NDPK-A (Song *et al.*, 2000). Therefore, in order to determine the crystal structure of fully oxidized NDPK-A, the concentrated protein solution was pre-incubated for 1 h with 10 m*M* H_2O_2. The stability of NDPK-A under these strongly oxidative conditions was monitored using a DynaPro 99 (Proterion Corporation, Piscataway, New Jersey, USA) to check for the formation of extremely high-molecular-mass aggregates indicating protein denaturation. NDPK-A was stable during incubation with 10 m*M* H_2O_2.

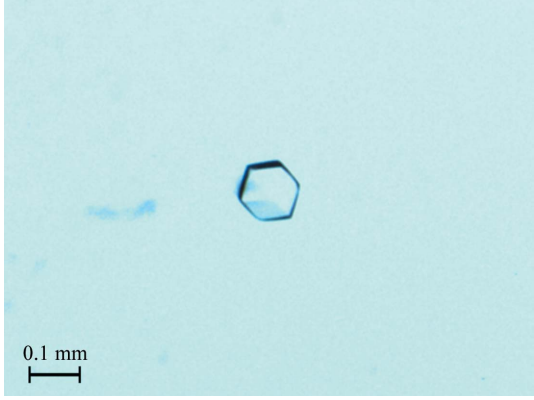

Figure 1
A cube-shaped crystal of oxidized NDPK-A.

Screening for crystallization conditions was performed using the sparse-matrix method (Jancarik & Kim, 1991) with several screens from Hampton Research (Laguna Niguel, California, USA). A Hydra Plus One crystallization robot (Matrix Technologies, Hudson, New Hampshire, USA) was used to set up the screens using the sitting-drop vapour-diffusion method at room temperature. A 96-well Intelli-Plate (Art Robbins Instruments, Salt Lake City, Utah, USA) was used and one sitting drop per well was made by mixing 0.2 µl protein solution (10 mg ml^{-1}) with 0.2 µl reservoir solution and was equilibrated against 90 µl reservoir solution. A VDX48 plate (Hampton Research, Laguna Niguel, California, USA) was used to optimize the crystallization conditions in hanging drops by mixing 0.8 µl protein solution and 0.8 µl reservoir solution containing 2.0 *M* sodium potassium phosphate pH 6.4 and equilibrating against 100 µl reservoir solution.

2.2. Data collection and reduction

Concentrated sodium formate solution was added to the well solution as a cryoprotectant to a final concentration of 1.4 *M*. Prior to flash-cooling in liquid nitrogen, crystals were soaked in the equilibrated well solution for 1 min. X-ray diffraction data were collected at a wavelength of 1 Å on beamline 4A at Pohang Light Source using a Quantum 4 CCD detector (Area Detector Systems Co., Poway, California, USA) placed at a distance of 300 mm from the sample. The oscillation range per image was 1.0° with 20 s exposure. 130 oscillation images were collected with no overlap between contiguous images. X-ray diffraction data were processed and scaled using *MOSFLM* and *SCALA* from the *CCP*4 program suite (Collaborative Computational Project, Number 4, 1994). The relatively high R_{merge} value of 17.3% in Table 1 arises from the high data multiplicity and the weak intensities of the reflections. Since the R_{merge} value gradually increases from 6.2% (between 50 and 8 Å resolution) to 57.7% (between 2.95 and 2.80 Å resolution), the high R_{merge} does not arise from a space-group issue.

3. Results and discussion

Diffraction-quality crystals were easily obtained using a reservoir solution consisting of 2.0 *M* sodium potassium phosphate pH 6.4. Crystals grew to dimensions of 0.07 × 0.07 × 0.07 mm within three weeks at 296 K (Fig. 1). Synchrotron data were collected to 2.80 Å resolution. The crystal belonged to the primitive cubic space group

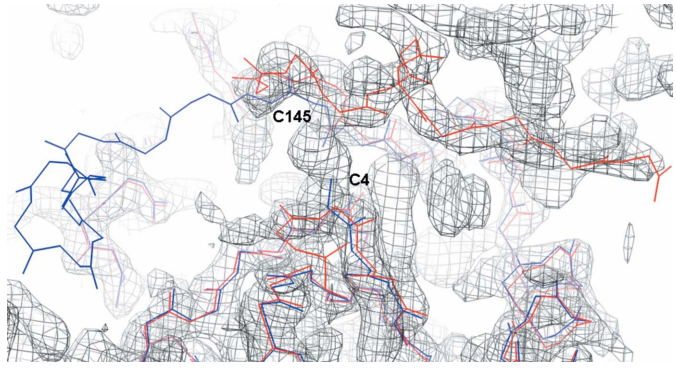

Figure 2
Preliminary electron-density map of oxidized NDPK-A. The $2F_o - F_c$ map around the disulfide bridge between Cys4 and Cys145 contoured at 2.0σ was drawn using initial phases calculated with all reflection data between 20 and 3.0 Å resolution. The backbones of the search model (blue) and the initial target model (red) are shown. This figure was generated using *UCSF Chimera* (Pettersen *et al.*, 2004).

$P2_13$, with unit-cell parameters $a = b = c = 106.8$ Å. Based on a Matthews coefficient estimation (Matthews, 1968), the asymmetric unit contains two NDPK-A subunits (V_M of 2.82 Å^3 Da^{-1} and solvent content of 56.4%). Details of the data-collection statistics are presented in Table 1.

Molecular replacement was performed to solve the phase problem. A good solution was found using a dimeric form composed of chains *A* and *B* of the native human NDPK-A crystal structure (PDB code 1jxv; Min *et al.*, 2002) as a search model with the *EPMR* program (Kissinger *et al.*, 1999). The initial *R* factor after rigid-body refinement was 0.471 using all data between 20 and 3.5 Å resolution. The unusually high *R* factor implies the presence of local conformational differences between the search model and the target molecules. As expected, the preliminary electron-density map revealed a large conformational change of the C-terminal domain of NDPK-A induced by an unexpected intramolecular disulfide bridge between Cys4 and Cys145 (Fig. 2). Since this conformational change influences the Kpn loop region essential for hexamerization and NDPK activity, it seems that the reduced activity of NDPK-A under oxidative conditions is strongly connected to destabilization of the hexameric state of NDPK-A. We generated a unit cell with a partially refined model to check whether oxidized NDPK-A forms a dimer in the crystal as shown in solution by size-exclusion chromatography (Song *et al.*, 2000). However, oxidized NDPK-A also packs as a hexamer in the unit cell. We suggest that the hexamer may be a crystallographic artifact composed of three biologically inactive dimers owing to the high protein concentration. It has been reported that a nonphysiological high-molecular-mass oligomer is also formed in the case of *Mycobacterium tuberculosis* AhpC owing to the high protein concentration (Hall *et al.*, 2009). Full structure determination is in progress in order to understand how the structure of oxidized NDPK-A influences its enzymatic activity during the oxido-reduction cycle.

We are grateful to the staff of Pohang Light Source. The work described here was supported by grant No. R15-2006-020 from the NCRC program of MOST and KOSEF through the CCS and DDR at Ewha Womans University. M-SK is supported by a Brain Korea 21 grant from the Ministry of Education and Human Resources Development.

References

Collaborative Computational Project, Number 4 (1994). *Acta Cryst.* D**50**, 760–763.
Hall, A., Karplus, P. A. & Poole, L. B. (2009). *FEBS J.* **276**, 2469–2477.
Ishikawa, N., Shimada, N., Takagi, Y., Ishijima, Y., Fukuda, M. & Kimura, N. (2003). *J. Bioenerg. Biomembr.* **35**, 7–18.
Jancarik, J. & Kim, S.-H. (1991). *J. Appl. Cryst.* **24**, 409–411.
Kissinger, C. R., Gehlhaar, D. K. & Fogel, D. B. (1999). *Acta Cryst.* D**55**, 484–491.
Lee, E., Jeong, J., Song, E. J., Kang, S. W. & Lee, K.-J. (2009). *PLoS One*, **4**, e7949.
Matthews, B. W. (1968). *J. Mol. Biol.* **33**, 6491–6493.
Min, K., Song, H. K., Chang, C., Kim, S. Y., Lee, K.-J. & Suh, S. W. (2002). *Proteins*, **46**, 340–342.
Otero, A. S. (2000). *J. Bioenerg. Biomembr.* **32**, 269–275.
Pettersen, E. F., Goddard, T. D., Huang, C. C., Couch, G. S., Greenblatt, D. M., Meng, E. C. & Ferrin, T. E. (2004). *J. Comput. Chem.* **25**, 1605–1612.
Rosengard, A. M., Krutzsch, H. C., Shearn, A., Biggs, J. R., Barker, E., Margulies, I. M., King, C. R., Liotta, L. A. & Steeg, P. S. (1989). *Nature (London)*, **342**, 177–180.
Song, E. J., Kim, Y. S., Chung, J. Y., Kim, E., Chae, S.-K. & Lee, K.-J. (2000). *Biochemistry*, **39**, 10090–10097.
Stone, J. R. & Yang, S. (2006). *Antioxid. Redox Signal.* **8**, 243–270.